



**TECHNICAL PAPER FOR STUDENTS AND YOUNG ENGINEERS**  
**- FISITA WORLD AUTOMOTIVE CONGRESS, BARCELONA 2004 -**

TITLE:

**TOWARDS THE OPTIMUM SOLUTION OF VEHICLE COMPATIBILITY:  
A NUMERICAL STUDY USING A FIXED SMART STRUCTURE**

Topic:

- FUTURE AUTOMOTIVE TECHNOLOGY       INTELLIGENT TRANSPORTATION SYSTEMS  
 USER FRIENDLY AUTOMOBILE       ADVANCED PRODUCTION AND LOGISTICS  
 VEHICLES & THE ENVIRONMENT

Author(s):

Elmarakbi, Ahmed\* and Zu, Jean

Nationality:

Canadian

University / Institution:

University of Toronto, Departement of Mechanical and Industrial Engineering

National Society:

- YES       NO

Name of the National Society:

Abstract:

The goal of this paper is to present mathematical models to investigate and to optimize crash compatibility. Since a slight softer crumple zone is required for heavier vehicles to improve the compatibility, a smart structure is proposed to support the function of the existing vehicle and to optimize vehicle compatibility. The proposed structure consists of two fixed independently hydraulic cylinders besides the longitudinal members in parallel position. The models of both standard-standard and smart-standard vehicles in head-on collision are developed and are numerically solved. It is proven from simulations that the smart vehicle brings significantly improvement in vehicle compatibility. In addition, it is shown that the models can be used in an effective way to give a quick insight of real life crashes.

Place / Date:

Toronto, 14/2/2004

**INTRODUCTION-** The crash compatibility of a vehicle is a combination of its crashworthiness and its aggressivity when involved in crashes with other members of the vehicle fleet. While the crashworthiness focuses on the capability of a vehicle to protect its occupants in a collision, aggressivity is measured in terms of the casualties to occupants of the other vehicle in the collision. Crashworthiness is sometimes referred to as self-protection while reduction in aggressivity is also referred to as partner-protection (1).

The topic of car compatibility has been studied as early as the 70's (1974) by Ventre (2), Kossar et al. (3), and Seffert (4) when the concept of car aggressivity emerged. For the period of (1974-1994) there was not much concern on compatibility but performance of restraint systems has been greatly improved (5). Despite publication of numerous research programs on compatibility, conflicting claims are being made regarding various factors affecting compatibility and aggressivity of road vehicles (6).

It is generally accepted that injury risk to the occupants is higher in lighter vehicle than larger one with which it is involved in head-on collision. However, because mass is a surrogate measure for other factors like size, shape, length of crumple zone and stiffness too, the effects of these individual factors on compatibility are overshadowed by the effect of mass (6). Conventional thinking tells us that when a smaller vehicle collides with a larger one, the occupant of the smaller vehicle usually fares worse. The smaller vehicle undergoes a higher velocity change, has less structure to absorb the crush and potentially has less interior space to mitigate the effect of occupant contact (7).

Vehicle-to-vehicle crash compatibility affects the vehicle passenger compartment's deceleration and intrusion, which are the two main causes of car occupant injuries. Studying the compatibility effect is required to set up safety priorities and to enhance occupant and partner protection. For this purpose, a simplified model is developed in this paper to study individual compatibility effect on occupant and partner protection. Additionally, an optimized mathematical model using a smart vehicle structure is developed and is used to evaluate the relative significance of the interactions among vehicle mass, stiffness and type of collisions. Moreover, the optimized mathematical model helps identify important compatibility factors and study their individual injury effects on crash safety. In this fashion, the difficulty of the compatibility issue is minimized. Furthermore, the mathematical models are able to predict both vehicle deceleration and local passenger compartment intrusion. It is shown that these models are valid, convenient, and simple, which supports its applicability and efficiency in compatibility research and can be useful in optimization studies.

**OPTIMIZATION OF VEHICLE COMPATIBILITY-** The front-end structures of two vehicles in head-on collision are used to protect the occupants of both vehicles. Due to the aggressive design of the large vehicles involved in a collision with smaller vehicle, the protection of the occupant of both small and large vehicles are conflicting each other. Only the large vehicle contributes toward its occupant protection. This leads to undesirable intrusions in the passenger compartment of the small vehicle. Moreover, most of real world frontal impacts involve partial overlap collision. Due to the physical nature of the frontal impact event, only one of the two longitudinal rail members contributes toward the energy absorption. This leads to undesirable intrusions in the passenger compartment. Excessive intrusion is usually generated on the impacted side subjecting occupants to injury risks. These injuries are more severe than the injuries generated during full frontal collision. Excessive intrusion and smooth deceleration of

occupants are the two most difficult parameters to be satisfied when designing for an offset crash event. These requirement challenges the safety engineers to seek an optimal design that maximizes the energy absorption capability of the crash zones, minimizes intrusion, and keeps occupant gravitational loads below the acceptable requirements.

To adapt structure design for crash conditions and compatibility issue, there is a need to develop a new structure concept. In addition, to decrease the aggressivity of the large vehicle towards the small vehicle, it is necessary to soften the front-end structure. This needs to use an additional energy absorber which can soften the larger vehicle front-end structure.

A new direction of crashworthiness improvement using smart structures is introduced to support the function of the existing vehicle structure. A smart structure system has been proposed to support the function of the existing vehicle structure. The proposed smart structure consists of two non-extendable hydraulic cylinders besides the longitudinal members in parallel position. The cylinders are fixed to the bumper, just like the front ends of the longitudinals. The load is distributed on both longitudinals using the hydraulic cylinders. If one of the longitudinals is loaded during an offset crash, the oil inside the loaded cylinder will move via a tube or a pipe to the cylinder of the unloaded side, forcing the other longitudinal to deform as well.

**MATHEMATICAL MODEL** - The simulation model presented in this paper is intended for a two-car collinear head-on collision. it is worthwhile mentioning that vehicle components, which significantly affect the dynamics of frontal impact, are modeled by lumped masses and nonlinear springs.

The model shown in Fig. 1 represents two vehicles, denoted as vehicle 1, which indicates the standard vehicle and vehicle 2, which represents the vehicle with new front – end structure. They impact each other at initial velocities  $v_1$  and  $v_2$ , respectively. The stiffness elements shown as springs with stiffness  $k_{ij}$  are the plastic deformation parts representing the longitudinal members. Dampers with damping coefficient  $c_k$  represent the hydraulic cylinders.

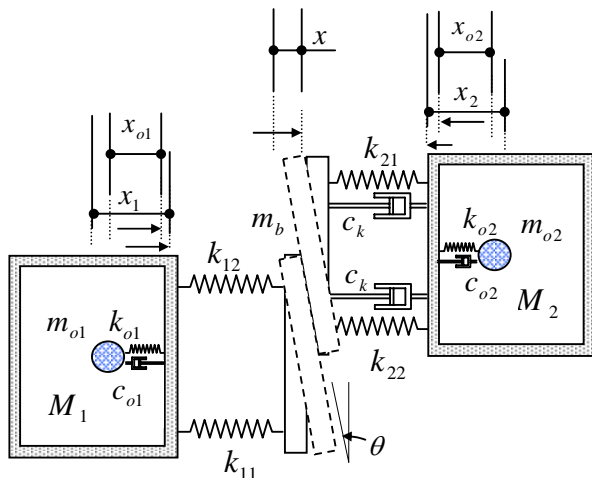


Fig. 1 Mathematical model of offset frontal collision

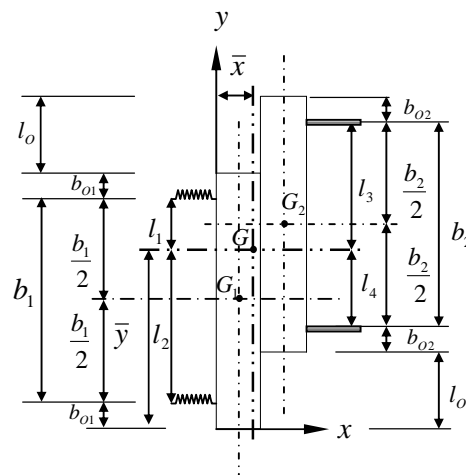


Fig. 2 Mathematical model of the bumper assembly ( offset collision )

The occupant's restraint characteristics of seat belt and airbag are represented by stiffness  $k_{oi}$  and damping coefficient  $c_{oi}$ . Moreover, the masses of the vehicle body and the occupant are defined by  $M_i$  and  $m_{oi}$ , respectively, as also shown in Fig. 1.

The two bumpers' masses (bumper assembly) shown in Fig. 2 stay together after impact (perfectly plastic impact) and have the same velocity and displacement. The velocity of the bumper assembly is calculated using the law of momentum interchange. In addition, the displacement of the bumper assembly is assumed to be zero. The mass of the bumper assembly is  $m_b$ .

In case of crash analysis, the mass is always constant, while the damping and stiffness are not; they mainly depend on the velocity and displacement values. In this paper, the forces of the plastic springs  $(F_s)_{ij}(\delta_{ij})$  and damping forces  $(F_d)_k(v_{dk})$  will be defined in the following form as

1. The forces of the plastic springs (piecewise linear) shown in Fig. 3 are defined as

$$(F_s)_{ij}(\delta_{ij}) = f_0 + (k_{ij})_1 \cdot \delta_{ij} \quad \delta_{ij} \leq \delta_{ij}^* \quad (1)$$

$$(F_s)_{ij}(\delta_{ij}) = f_0 + (k_{ij})_1 \cdot \delta_{ij}^* + (k_{ij})_2 \cdot (\delta_{ij} - \delta_{ij}^*) \quad \delta_{ij} > \delta_{ij}^* \quad (2)$$

2. The damping forces (piecewise linear) shown in Fig. 4 are given by

$$(F_d)_k = (c_k)_1 \cdot v_k \quad v_k \leq v_{dk}^* \quad (3)$$

$$(F_d)_k = (c_k)_1 \cdot v_{dk}^* + (c_k)_2 \cdot (v_k - v_{dk}^*) \quad v_k > v_{dk}^* \quad (4)$$

where  $i = 1,2$  (represent the first and second vehicle, respectively).

$j = 1,2$  (represent right and left rail, respectively).

$k = 1,2$  (represent right and left hydraulic cylinder, respectively).

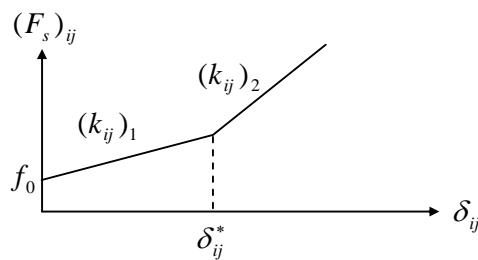


Fig. 3 Force - deformation characteristic

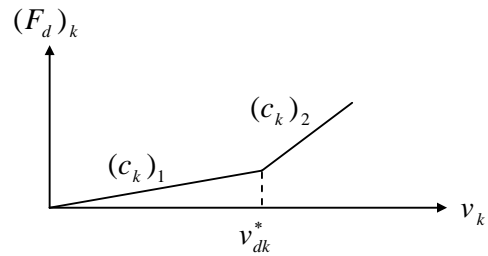


Fig. 4 Force - velocity characteristic

3. The force generated by the spring on the occupant is expressed as

$$(F_{so})_i = 0 \quad \delta_{oi} \leq \delta_{c_{oi}} \quad (5)$$

$$(F_{so})_i = k_{oi} \cdot (\delta_{oi} - \delta_{c_{oi}}) \quad \delta_{oi} > \delta_{c_{oi}} \quad (6)$$

where  $\delta_{c_{oi}}$  is the initial slack length. The slack length represents the relative displacement of the occupant  $\delta_{oi}$  before the seatbelt becomes effective. The damping

coefficient of the restraint system is taken as 50% of the critical damping. In addition, the damping force on the occupant is given by

$$(F_{do})_i = c_{oi} \cdot v_{oi} \quad (7)$$

**DYNAMIC RESPONSE OF VEHICLE COMPATIBILITY** - The goal of this section is to analyze vehicle compatibility and to find the dynamic response, deformation and declaration, of the vehicle and the occupant involved in a collision. In this section, the numerical solutions of the mathematical models are given in both full and offset frontal collision cases of smart structures with piecewise characteristics.

## VEHICLE -TO - VEHICLE IN FRONTAL COLLISION

### Dynamic Response

The initial collision event when a vehicle hits an obstacle (barrier, vehicle, etc.) is referred to as the first or primary impact. The following event when the occupant moves within the vehicle and impacts the interior is called the secondary impact.

#### Primary Impact

The equations of motion of vehicle-to-vehicle in frontal collision model shown in Fig. 1 can be written as

$$m_b \cdot \ddot{x} + F_{d1}(v_{d1}) + F_{d2}(v_{d2}) + F_{22}(\delta_{22}) + F_{21}(\delta_{21}) - F_{11}(\delta_{11}) - F_{12}(\delta_{12}) = 0 \quad (8)$$

$$M_1 \cdot \ddot{x}_1 + F_{11}(\delta_{11}) + F_{12}(\delta_{12}) = 0 \quad (9)$$

$$M_2 \cdot \ddot{x}_2 + F_{d1}(v_{d1}) + F_{d2}(v_{d2}) + F_{22}(\delta_{22}) + F_{21}(\delta_{21}) = 0 \quad (10)$$

$$I \cdot \ddot{\theta} + F_{12}(\delta_{12}) \cdot l_1 - F_{11}(\delta_{11}) \cdot l_2 + [F_{d2}(v_{d2}) + F_{22}(\delta_{22})] \cdot l_4 - [F_{d1}(v_{d1}) + F_{21}(\delta_{21})] \cdot l_3 = 0 \quad (11)$$

#### Secondary Impact

The equations of motion of the occupant can be written as

$$m_{o1} \cdot \ddot{x}_{o1} + F_{so1}(\delta_{o1}) + F_{co1}(v_{o1}) = 0 \quad (12)$$

$$m_{o2} \cdot \ddot{x}_{o2} + F_{so2}(\delta_{o2}) + F_{co2}(v_{o2}) = 0 \quad (13)$$

where the deformations of the plastic springs of the longitudinals and the relative displacements of the occupants are defined respectively as follows:

$$\delta_{11} = x_1 - x_{11}, \delta_{12} = x_1 - x_{12}, \delta_{22} = x_2 + x_{22}, \delta_{21} = x_2 + x_{21} \quad (14)$$

$$\delta_{o1} = x_{o1} - x_1, \delta_{o2} = x_{o2} - x_2 \quad (15)$$

The displacements of the spring ends are given by

$$\left. \begin{aligned} x_{11} &= x + l_2 \cdot \tan \theta & x_{21} &= x - l_3 \cdot \tan \theta \\ x_{12} &= x - l_1 \cdot \tan \theta & x_{22} &= x + l_4 \cdot \tan \theta \end{aligned} \right\} \quad (16)$$

The velocities of the hydraulic cylinders and relative velocities of the occupants are defined respectively as

$$v_1 = \dot{x}_2 + \dot{x}_{21}, v_2 = \dot{x}_2 + \dot{x}_{22} \quad (17)$$

$$v_{o1} = \dot{x}_{o1} - \dot{x}_1, v_{o2} = \dot{x}_{o2} - \dot{x}_2 \quad (18)$$

and the velocities of the hydraulic cylinders ends are defined as

$$\dot{x}_{21} = \dot{x} - l_3 \cdot \sec^2 \theta \dot{\theta}, \dot{x}_{22} = \dot{x} + l_4 \cdot \sec^2 \theta \dot{\theta} \quad (19)$$

**SIMULATIONS** - In this section the analysis developed in the former section is verified by the presentation of the results for the mathematical model. The injury severity criteria are used to interpret the results. To compare the injury severity criteria for different vehicle collisions, some kind of index or formula is needed.

The main injury severity criterion of interest in this paper is the intrusion criterion, which denotes the interior deformation of the vehicle structure and its effects on the passenger compartment. High impact speeds may result in more severe injuries to vehicle occupants. The intrusion levels depend on how the vehicle structure is assembled and how the impact energy is absorbed by the vehicle structure. The intrusion injury criterion measured as the maximum deformation suffered by the longitudinal members. The second injury criterion that has been considered is the deceleration level of the occupant which measured as the maximum deceleration pulse sustained by the occupant during the crash event.

Numerical simulations have been used as a tool to demonstrate the influence of various crash situations on the energy absorbed by the proposed structure. The central difference method is used to solve the differential Eqs. (8-13). The initial conditions are specified as

$$x_1(0) = x_2(0) = x_{o1}(0) = x_{o2}(0) = 0, v_1(0) = v_2(0) = v_{o1}(0) = v_{o2}(0) = v_i \quad (20)$$

The following data are used in the numerical solution. The mass of vehicle 2 is  $M_2 = 1500$  kg, and the mass of vehicle 1 is  $M_1$  ranges from  $2M_2$  to  $0.1M_2$ . Moreover, the mass of the bumper assembly is  $m_b = m_{b1} + m_{b2}$ ,  $m_{b2} = 50$  kg and  $m_{b1}$  varies from  $2m_{b2}$  to  $0.1m_{b2}$ . The force-deformation characteristic for each longitudinal member for vehicle 2 is shown in Fig. 3 with the following values:  $(k_{ij})_1 = 250$  kN/m,  $(k_{ij})_2 = 450$  kN/m, and  $\delta_{dk}^* = 0.1$  m. In addition, the values for vehicle 1 range from  $2k_{ij}$  to  $0.1k_{ij}$ . The damping coefficient of the hydraulic cylinder characteristics are as follows:  $(c_k)_1 = 10$  kN.s/m,  $(c_k)_2 = 12.5$  kN.s/m, and  $v_{dk}^* = 7$  m/s. The mass of the occupant is  $m_{oi} = 70$  kg for both vehicles. Furthermore, the occupant's restraint characteristics of the seat belt and the airbag are represented by stiffness  $k_{oi} = 98.1$  kN/m and damping coefficient  $c_{oi} = 2.54$  kN.s/m. The initial velocity for both vehicles is  $v_i = 13.33$  m/s. The bumper assembly dimensions are  $b_i$  and  $b_{oi} = 0.9$  and  $0.3$  m, respectively.

## MASS EFFECT

The aim of this simulation is to compare the performance of the smart vehicle structure in full and offset frontal collisions and to improve vehicle compatibility. Two sets of simulation runs involving two vehicles in head-on collision are used. The first set involves a collision of smart vehicle (SM) with standard vehicle (ST). The second set involves a collision of two identical standard vehicles (ST). The first factor investigated is the mass ratio. Figs. 5 and 6 show the variation of injury criteria with the mass ratio  $M_2 : M_1$  ranging from 0.5 -10. The stiffness ratio  $k_{ij_2} : k_{ij_1}$  is assumed = 1 for both vehicles while the overlap is taken to be 100 % (full front collision). The aggressivity is measured on changes in injury criteria of the vehicle 2 due to variation in characteristics of the partner vehicle 1.

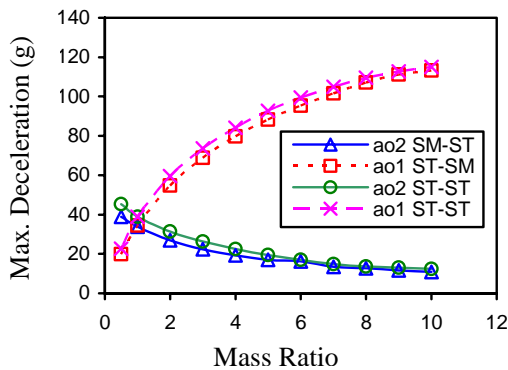


Fig. 5 Max. deceleration versus mass ratio (full collision)

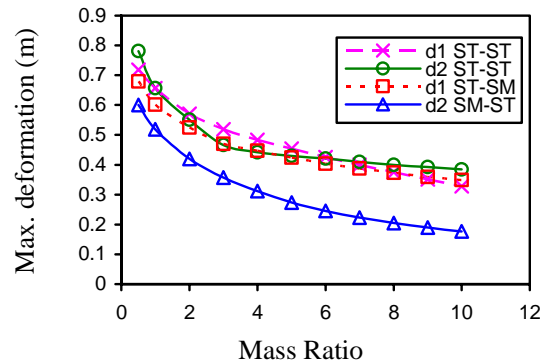


Fig. 6 Max. deformation versus mass ratio (full collision)

Fig.5 shows a slight reduction of the occupant deceleration. The results of the second injury criteria, deformation length, are also determined in the case of full frontal collision. Fig.6 clearly shows the reduction in intrusion injury in full collision. This can be concluded by noting that the deformation of the smart vehicle increases from 0.17 m at ratio 10 to 0.6 m at ratio 0.5 and the deformation of the partner vehicle increases from 0.35 m at ratio 10 to 0.68 m at ratio 0.5 while in the standard collision, the deformation of vehicle 2 increases from 0.39 m at ratio 10 to 0.78 m at ratio 0.5 and the deformation of vehicle 1 increases from 0.33 m at ratio 10 to 0.72 m at ratio 0.5.

The same results are also gained in the case of 50% offset frontal collision for both sets of simulations. The reduction of intrusion injury in offset collision can be concluded by noting that for the deformation of the smart vehicle increases from 0.30 m at ratio 10 to 0.84 m at ratio 0.5 and the deformation of the partner vehicle increases from 0.35 m at ratio 10 to 0.91 m at ratio 0.5 while in the standard collision, deformation of vehicle 2 increases from 0.44 m at ratio 10 to 1.04 m at ratio 0.5 and the deformation of vehicle 1 increases from 0.39 m at ratio 10 to 1.14 m at ratio 0.5. Moreover, there is a slight reduction of the occupant declaration.

## STIFFNESS EFFECT

The second factor investigated is the stiffness ratio. Figs. 7 and 8 show the variation of the injury criteria with the stiffness ratio ranging from 0.5 - 10. The maximum ratio of 10 is dictated by the maximum possible rigid structure. The mass ratio is assumed = 1 for both vehicles while the overlap is taken to be 100 %. Again the aggressivity is

measured on changes in injury criteria of the vehicle 2 due to variation in characteristics of the partner vehicle 1.

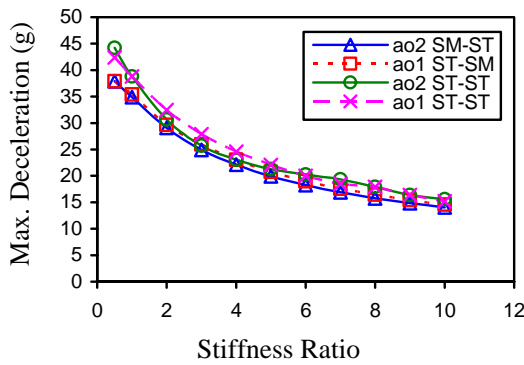


Fig. 7 Max. deceleration versus stiffness ratio (full collision)

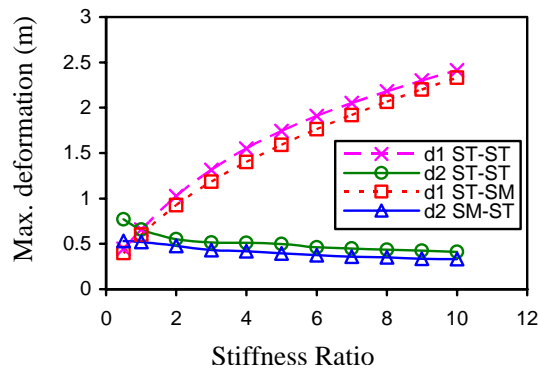


Fig. 8 Max. deformation versus stiffness ratio (full collision)

It is worthwhile noting that there is a reduction of the occupant deceleration in the case of smart collision. The deceleration of the smart vehicle's occupant increases from 14 g at ratio 10 to 38 g at ratio 0.5 compared to the partner's vehicle occupant which increases from 14.5 g at ratio 10 to 38 g at ratio 0.5 while in the standard collision, the occupant deceleration of vehicle 2 increases from 15.6 g at ratio 10 to 44 g at ratio 0.5 and the occupant deceleration of vehicle 1 increases from 15.2 g at ratio 10 to 42 g at ratio 0.5. For 50% overlap, the stiffness ratio has a level of deceleration aggressivity smaller than that for the 100% overlap.

Intrusion reductions are clear from Fig. 8 for full collision, which shows a significant reduction on the deformation of the standard vehicle in head on collision with the smart vehicle. This can be concluded by noting that the deformation of smart vehicles decreases from 0.53 m at ratio 0.5 to 0.33 m at ratio 10, compared to the deformation of the partner vehicles which increases from 0.4 m at ratio 0.5 to 2.33 m at ratio 10 while in the case of standard collision, the deformation of vehicle 2 decreases from 0.77 m at ratio 0.5 to 0.41 m at ratio 10 and the deformation of vehicle 1 increases from 0.45 m at ratio 0.5 to 2.41 m at ratio 10. This means that by integrating the smart structure in the front end design of large vehicle, the deformation and the deceleration of the occupants of smaller vehicle are minimized.

#### COMBINED MASS AND STIFFNESS EFFECT

The mass and stiffness ratios have proved to demonstrate enhanced aggressivity results regarding deformation and deceleration criteria. In this simulation, the mass and stiffness ratios are both ranging from 0.5 -10. Vehicle 2 has fixed characteristics while vehicle 1 has varied characteristics. Figs. 9 and 10 show a significant improvement for both criteria. The reduction of the deceleration is clear form Fig. 9. The reduction of intrusion injury can be seen from Fig. 10 by noting that for the deformation of the smart vehicle increases from 0.13 m at ratio 10 to 0.62 m at ratio of 0.5 and the deformation of the partner vehicle decreases from 1.02 m at ratio 10 to 0.42 m at ratio 0.5 while in the standard collision, the deformation of vehicle 2 increases from 0.185 m at ratio 10 to 0.86 m at ratio 0.5 and the deformation of vehicle 1 decreases from 1.10 m at ratio 10 to 0.48 m at ratio 0.5. The same results are also obtained in the case of 50% offset

collision. In summary, the significant improvements of both intrusion and deceleration injuries in the cases of full and offset collisions are obtained using the smart structures. In addition, it is shown that the mathematical models can be used in an effective way to give a quick insight in the basics of real life crashes.

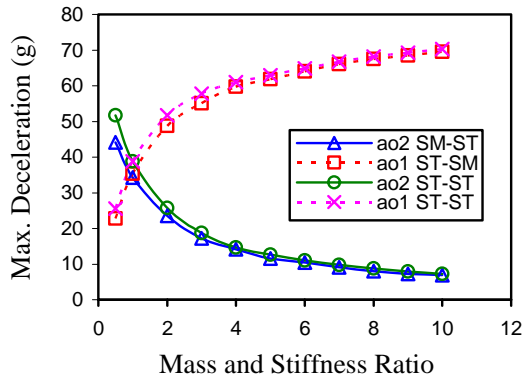


Fig. 9 Max. deceleration versus mass and stiffness ratio (full collision)

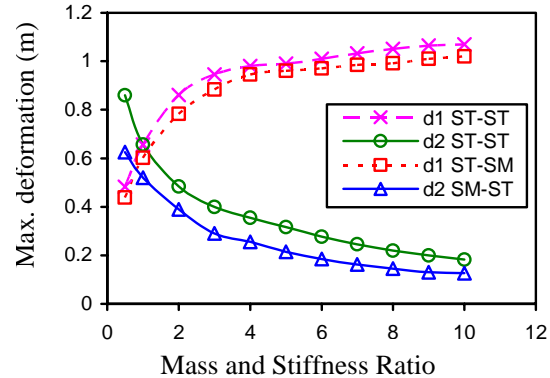


Fig. 10 Max. deformation versus mass and stiffness ratio (full collision)

**CONCLUSIONS-** Compatibility is a crucial issue, which is difficult to measure using a single parameter such as mass or stiffness. A slightly softer crumple zone is required for heavier vehicles to achieve this compatibility. This can be achieved using a smart structure with two non-extendable hydraulic cylinders integrated within the front-end structure. The mathematical models for both standard and smart vehicle frontal collisions are developed and are numerically solved. It is proven from numerical simulations that the smart structure involved in head-on collision with standard vehicle surpasses the traditional structure concept in absorbing crash energy for the same crash distance. Moreover, it is shown that these models are valid, and flexible, which supports its applicability and efficiency in crash research and can be useful in optimization studies.

## REFERENCES

- (1) Galber H., Hollowell W., and Summers S., "Systems Modelling of Frontal Crash Compatibility", SAE No. 2000-01-0878, 2000.
- (2) Ventre P., "Compatibility between Vehicles in Frontal and Semi- Frontal Collisions", 5th ESV Conference, London, England, June 4-7, 1974.
- (3) Kossar J., "Big and Little Car Compatibility." 5th ESV Conference, London, England, June 4-7, 1974.
- (4) Seffert U., "Compatibility on the road." 5th ESV Conference, London, England, June 4-7, 1974.
- (5) Tarriere C., Morvan Y., Steyer C., and Bellot D., "Accident research and experimental data useful for an understanding of the influence of Car Structural Incompatibility on the Risk of Accident Injury." 14th ESV Conference, Munich, Germany, May 23-26, 1994.
- (6) Jawad, S., Mahmood, H., and Baccouch, M., "Smart Structure for Improving Crashworthiness in Vehicle Frontal Collisions." The ASME Mechanical Engineering Congress and Exposition, Nashville, Tennessee, USA, November 14-19, 1999.
- (7) Shearlaw, A., and Thomas, P., "Vehicle-to-Vehicle Compatibility of Vehicles in Real World Accidents" 15th ESV Conference, Melbourne, Australia, May 13-17, 1996.